INSTITUTE OF PHYSICS PUBLISHING MEASUREMENT SCIENCE AND TECHNOLOGY

Meas. Sci. Technol. **18** (2007) 155–160 doi:10.1088/0957-0233/18/1/019

# Timing resolution (FWHM) of some photon counting detectors and electronic circuitry

**P Jani, L Vámos and T Nemes**

Research Institute for Solid State Physics and Optics, PO Box 49, H-1525 Budapest 114, Hungary

E-mail: pjani@sunserv.kfki.hu

Received 19 September 2006, in final form 2 November 2006
Published 30 November 2006
Online at stacks.iop.org/MST/18/155

**Abstract**
An improved measurement scheme is proposed for the timing resolution of some commercially available photon detecting and counting APDs. The statistics of the time intervals corresponding to time of flight through passive media was recorded. Consequences of intrinsic photon arrival time ambiguity are taken into account. This improved scheme leads to better timing resolutions than claimed by the manufacturers. In one exemplary case the mean value is 31.2 ps instead of 40 ps.

**Keywords:** timing resolution, photon counting detectors, APD

## 1. Introduction

In many practical applications the knowledge of the timing resolution, or as it is called the timing jitter, of photon counting detectors and their amplifying signal conditioning electronic circuitry is fundamental, either because it is the basic data for the characterization of the ongoing physical or chemical process or because it imposes accuracy limits for measurement of other physical quantities. A case at hand is the fluorescent decay of organic materials or biological or chemical sensing. The timing resolution is characterized by the full width at half maximum (FWHM) of the response to a given time interval event. The statistical fluctuation of the time interval between the arrival photon at the sensor and output pulse leading edge is defined as the timing resolution or the timing jitter [1].

Continuous improvement in avalanche photo diode (APD) manufacturing technology and the comparative ease of use make APD detectors the almost exclusively used devices in photon counting experiments [2]. Although timing resolution is an essential property of detectors it is often missing from the specifications list or at best it can be deduced from manufacturers' application notes, see for example [3]. A possible source of error in this and other measuring schemes is that the timing resolution is measured between the source generating synchronization pulse and the detector response, meaning that the light-generating statistics are inherently involved in the measurement.

Our applied and proposed method is instead based on the measurement of time of flight (TOF) of light and electronic pulses through passive propagating media, fibre optical cable and low loss high frequency coaxial cable. The time of flight through these passive media is most stable with regard to temperature changes and external electrical disturbances. Earlier a very sophisticated method of timing resolution for avalanche diodes was proposed by [4], which is based on the simultaneous measurement of two avalanche diodes as a combined system. Using this method no separate data are available for a single avalanche diode.

This refined measurement scheme leads to better timing resolutions than sometimes claimed by the manufacturers.

A discussion is included concerning the intrinsic photon arrival time ambiguity when less than 200 ps pulse duration laser light is used in the experiment.

## 2. Theory

It is assumed throughout this paper that the propagation of errors is governed by independent uncorrelated sources whereby the square of the measured uncertainty ($\Delta X$) is the sum of the squares of the component uncertainties

$$(\Delta X)^2 = (\Delta A)^2 + (\Delta B)^2 + (\Delta C)^2, \quad (1)$$

where $\Delta A$ is the uncertainty of the time-measuring electronics, $\Delta B$ is the uncertainty of the signal conditioning electronics and $\Delta C$ is the intrinsic uncertainty of the APD.

  

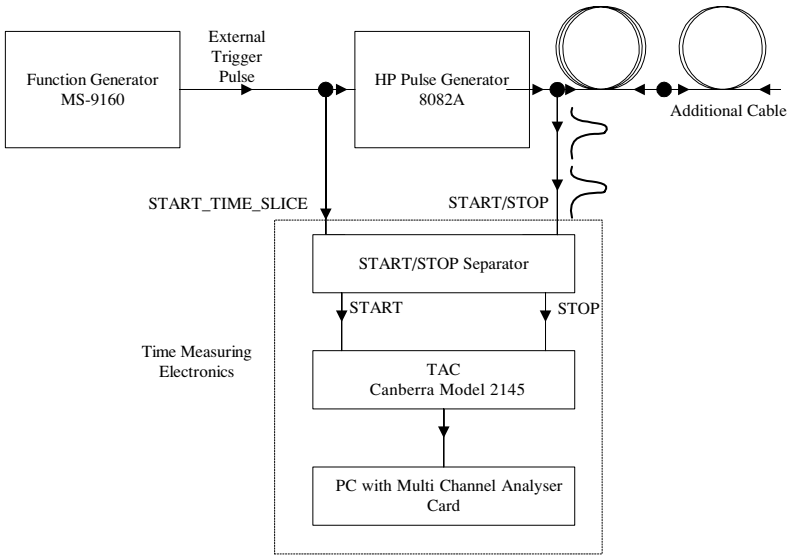


**Figure 1.** Block diagram of the test for time-measuring electronics.

So e.g. to define the timing resolution of the combined APD + signal conditioning electronics it is enough to measure the timing resolution of the combined system ($\Delta X$), and subtract from it the value of time-measuring electronics $\Delta A$

$$\Delta D = \sqrt{(\Delta B)^2 + (\Delta C)^2} = \sqrt{(\Delta X)^2 - (\Delta A)^2}. \qquad (2)$$

## 3. Experimental setup

Three different experimental setups were used in these measurements:

(1) Test of time-measuring electronics ($\Delta A$).
(2) Measurement of the timing resolution of the combined APD + signal conditioning electronics ($\Delta D$).
(3) Measurement of the timing resolution of the signal conditioning electronics ($\Delta B$).

### *3.1. Test of time-measuring electronics (ME)*

The block diagram to define the timing resolution of the time-measuring electronics is shown in figure 1. It consists of a START/STOP separator, a CANBERRA time to amplitude converter (TAC) [4], Model 2145 and a PC multi channel analyser (MCA) card.

Our proposed technique is very similar to that used in time-domain reflectometry (TDR), modified to the conditions of the specific experiment. It is proposed to measure the time intervals which are generated by signals and their reflections from a free cable end. The goal of using only passive elements for the generation of time intervals implies that these signals appear on the same electronic line. For this purpose a START/STOP separator unit was constructed. As its name suggests, it separates the consecutive input signals either to the START or STOP inputs of the TAC. These signals determine the beginning and the end of the time period to be measured. The main functional building blocks of circuitry are shown in figure 2.

The START_TIME_SLICE signal plays an important role in the timing of the separator. Responding to the START_TIME_SLICE signal the separator starts a time window in which it receives a pair of pulses and handles them. The first is directed to the START input of the TAC, the second is directed to the STOP input of the TAC. The STOP signal closes that window. That is, the separator unit interprets the first two pulses coming in after a START_TIME_SLICE signal as START and STOP signals to the TAC. After this cycle it gets into its stand-by state and waits for the next START_TIME_SLICE signal. Using this method the effect of noise-related signals can be significantly decreased, e.g. shot noise events, systematic reflections.

To measure well-defined time intervals we used signals of a high quality pulse generator (HP Pulse generator 8082A). This signal was fed to the START/STOP input of the separator and to a high frequency coaxial cable with a free end. The reflection from this free end served as the STOP signal for time measurement.

Two further considerations were taken into account. The cable length should be chosen such that the reflection comes late enough not to fall into the pulse width of the generator signal (approximately 10 ns). Second, the time interval should fall into the most sensitive range of the TAC—10 V/20 ns. For this reason a cable length of 101 cm was chosen.

Using an auxiliary pulse generator as an external trigger source (Voltcraft MS-9160) the time interval distribution between a signal and its reflected version was collected.

To determine the measuring range of the TAC and the resolution (ps/channel) of the MCA a small cable of 20 cm length was added to the free end of the reflection cable. The additional propagation delay is assumed to be 2.02 ns. A frequency distribution of time intervals for these two cases is shown in figure 3. From the plot it can be deduced that the channel widths of the time-measuring electronics are 2.71 ps/ch.

By simple curve-fitting techniques it was established that the timing resolution (FWHM) of the measuring electronics is $\Delta A_{ME} = 16.4$ ps.

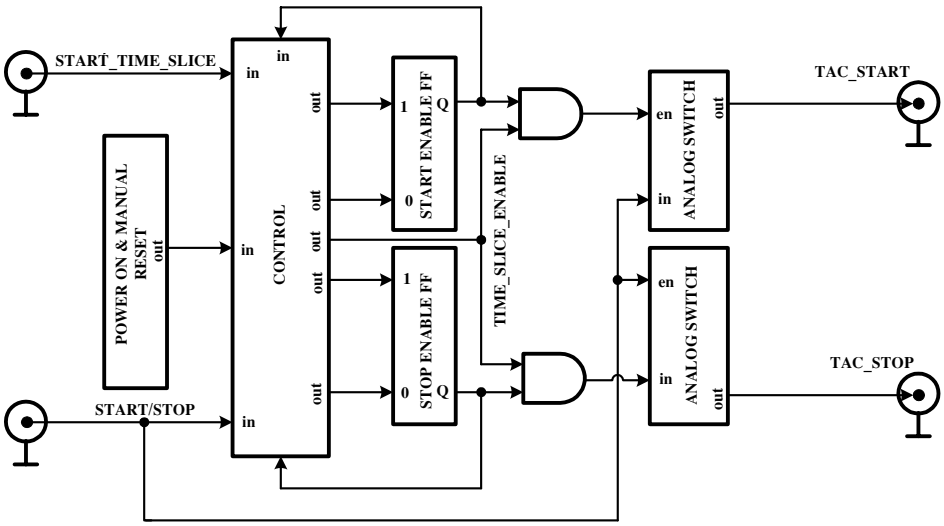


**Figure 2.** Block diagram of the START/STOP separator.

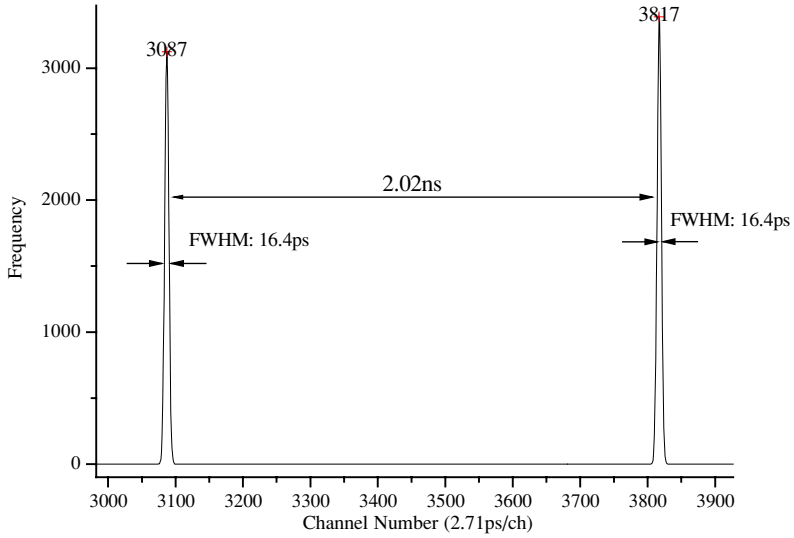


**Figure 3.** Frequency distribution of time intervals for measuring electronics.

### *3.2. The measurement of the timing resolution of the combined APD + signal conditioning electronics*

These measurements were performed following the block scheme shown in figure 4.

A HORIBA JOBIN YVON Pulsed NanoLED light source was used. It is claimed by the manufacturer that the pulse duration of the source is less than 200 ps, typically 100 ps. After appropriate neutral density filtering the light is launched into a Y-type fibre splitter of 50 $\mu$m core diameter achieving in this way an approximate 50–50 separation. One arm is connected to a second Y-type fibre splitter of the same type (FontCanada PO6302), used in this instance as a beam combiner. This is called the short arm. The other output of the splitter is connected to a long fibre of the same core diameter of 22 m geometrical length.

In this way each light pulse is sensed by the detector as two separate pulses—the time interval between them being the time of flight through the long fibre. The fibre length was chosen such that the separation between the pulses was surely larger than the dead time/pulse width of the detectors subsequently used.

To fall into the same highest sensitivity range of the TAC, a 23.7 m coax delay line was introduced into the START input of the TAC. Frequency distributions of time intervals for three different detector systems were collected, such as

(a) id100-20 of id Quantique,
(b) C5331-03 module of Hamamatsu and
(c) Si APD S2383 of Hamamatsu [6] combined with LABS29E signal conditioning electronics manufactured in our institute.

A frequency distribution of time intervals for the case of detector id100-20 of id Quantique is shown in figure 5. An additional propagation delay line of 15 cm length is introduced causing 802 ps additional delay to define the channel width and the timing resolution ($\Delta X$) value.

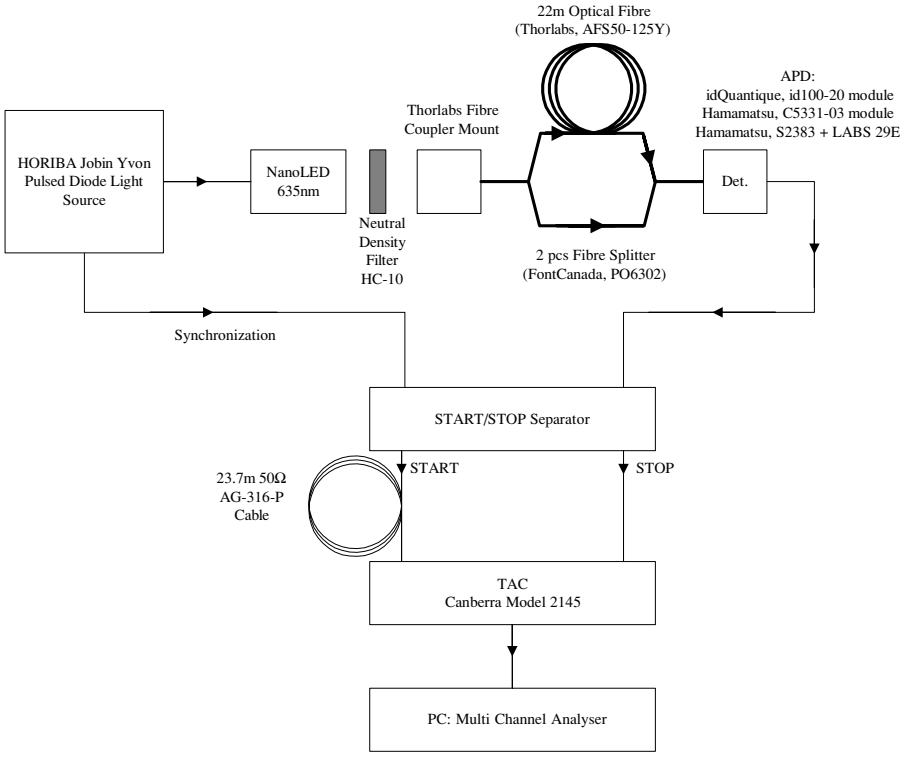


**Figure 4.** Measurement of the timing resolution of the combined APD + signal conditioning electronics.

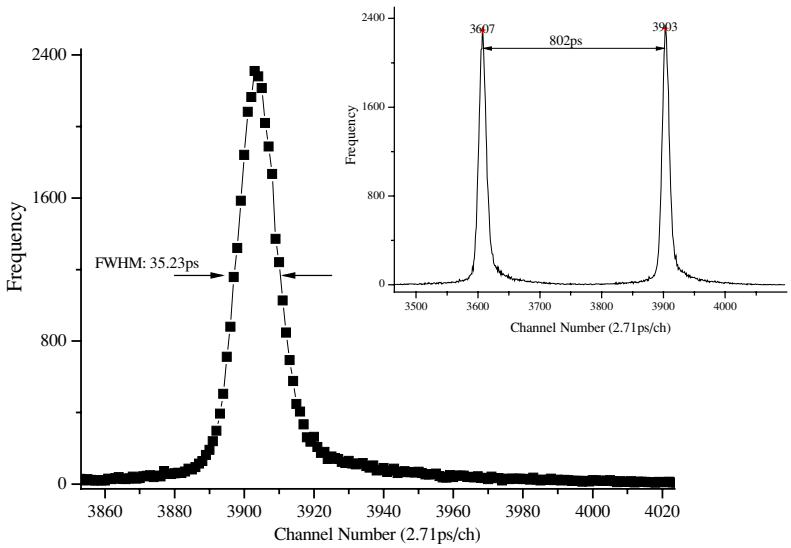


**Figure 5.** Frequency distribution of time intervals for the case of detector id100-20 of id Quantique.

### *3.3. Measurement of the timing resolution of the signal conditioning electronics*

In the case of (c) it was possible to determine the intrinsic timing resolution of the APD by measuring the LABS29E signal conditioning electronics separately.

The block diagram of LABS29E signal conditioning electronics is shown in figure 6. The dc/dc converter is a high voltage power supply for the APD. An amplifier receives the APD output signal and propagates to the restorer (RES) and to the constant fraction discriminator (CFD). The output ECL signal of the CFD can be translated optionally to NIM or TLL standard.

The timing resolution measurement of LABS29E signal conditioning electronics was performed according to the block diagram shown in figure 7.

It is seen that this measurement is almost exactly the same as that of the time-measuring electronics, with the difference that the detector electronics is fed with the START/STOP line and its output is fed into the START/STOP separator. The APD

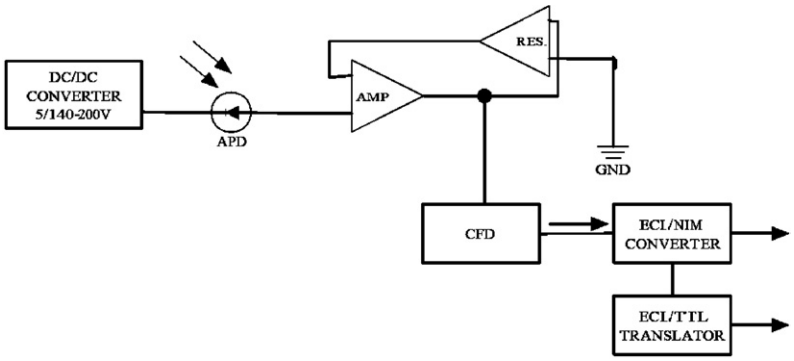


**Figure 6.** Block diagram of the LABS29E signal conditioning electronics.

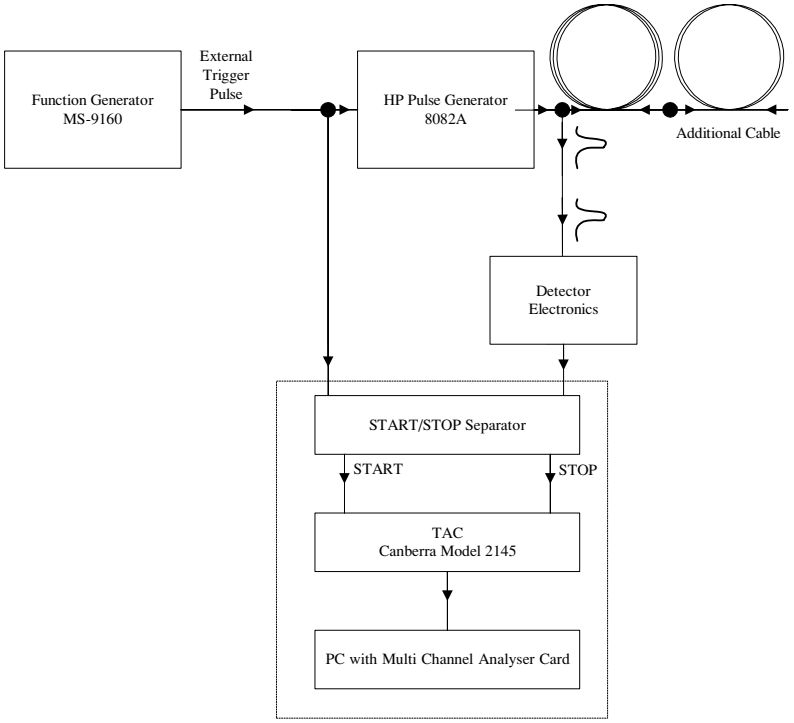


**Figure 7.** Measurement of the timing resolution of LABS29E signal conditioning electronics.

is disconnected in this case. We found that the value of the timing resolution of LABS29E signal conditioning electronics was equal to

$$\Delta B_{\mathrm{LAB29E}} = \sqrt{(\Delta X)^2 - (\Delta A_{ME})^2} = 27.1 \text{ ps}. \qquad (3)$$

Since the APD is not present in this experiment, $\Delta C = 0$.

## 4. Results and discussion

The timing resolution of the detector id100-20 of id Quantique was found to be (figures 3 and 5)

$$\Delta D_{\mathrm{id100-20}} = \sqrt{(35.23)^2 - (16.4)^2} = 31.18 \text{ ps}.$$

This result is much better than that claimed by the manufacturers in their technical note cited above. Their typical value was $\Delta D_{\mathrm{id100\text{-}20}} = 40$ ps (FWHM) [4].

The timing resolution of the detector C5331-03 module of Hamamatsu was found to be $\Delta D_{\mathrm{C5331\text{-}03}} = 147.1$ ps.

This parameter is not indicated in the specifications.

We measured the timing resolution of three Si APD S2383 detectors with the following serial numbers: SN NB 6242, SN NB 6254, SN NB 6264.

Each detector was set to the photon counting regime (Geiger mode) at the same operating temperature, $T = 21\ ^{\circ}\mathrm{C}$, maintained to $\pm 0.05\ ^{\circ}\mathrm{C}$ in a Peltier thermostat. The typical breakdown voltage of these detectors is $V_{\mathrm{br}} = 150$ V. These are manufacturer's data. We applied the following operating voltages: $U_{\mathrm{SNNB6242}} = 158.2$ V, $U_{\mathrm{SNNB6254}} = 162.8$ V, $U_{\mathrm{SNNB6264}} = 161.7$ V, meaning that the excess bias voltage of $V_{\mathrm{exbv}} = 8$–$12$ V was applied. This condition was chosen, somewhat arbitrarily, to provide equal mean dark count rate ($\overline{N}_d = 12$ cps) in all three devices.

Taking into account the timing resolution of LABS29E signal conditioning electronics by formula (1) it was found that

$$\Delta C = \sqrt{(\Delta X)^2 - (\Delta A_{ME})^2 - (\Delta B_{\mathrm{LAB29E}})^2}, \qquad (4)$$

$\Delta C_{\mathrm{SNNB6242}} = 236.9$ ps, $\Delta C_{\mathrm{SNNB6254}} = 156.8$ ps, $\Delta C_{\mathrm{SNNB6264}} = 204.2$ ps.

It is seen that there is a significant dispersion in the values although the serial numbers indicate close manufacturing.

To exclude further sources of error in our measurement we analysed the effect of photon arrival ambiguity. For this purpose we measured the average power of 1 MHz pulse train. From these data the average number of photons in a single pulse was computed. This measurement was performed with the THORLABS PM 120 Optical Power Meter System which has NIST calibration traceability. It was found that using a 100 times attenuation neutral density filter the pulse train average power for the short arm was $I_{\mathrm{short}} = 0.39$ nW and for the long arm $I_{\mathrm{long}} = 0.29$ nW. Converting these values to photon numbers with wavelength $\lambda = 635$ nm, it follows that in the worst case of 200 ps pulse length photons are separated by around 1 ps mean time. This means that photon arrival statistics plays no appreciable role in these experiments. Our forecast is that the same timing resolution results should be found in the case of femtosecond lasers. To verify this prediction we plan to repeat these experiments with femtosecond lasers.

## Acknowledgments

The authors wish to thank Zsolt Zárándi for his help and assistance in the design of the electronic circuitry and in the performance of the experiments.

## References

[1] Niclass C, Rochas A, Besse P A and Charbon E 2005 Design and characterization of a CMOS 3-D image sensor based on single photon avalanche diodes *IEEE J. Solid State Circuits* **40** 1847–54

[2] Dautet H, Deschamps P, Dion B, MacGregor A D, MacSween D, McIntyre R J, Trottier C and Webb P P 1993 Photon counting techniques with silicon avalanche photo diode *Appl. Opt.* **32** 3894–900

[3] Cova S, Lacaita A, Ghioni M and Ripamonti G 1989 20-ps timing resolution with single-photon avalanche diodes *Rev. Sci. Instrum.* **60** 1104–10

[4] Becker W 2005 Performance of the id100-20 detector in B&H TCSPC Systems *Beckel&Hickl GmBH Evaluation Note* http://www.becker-hickl.com

[5] Canberra Industries An introduction to time correlated single photon counting for fluorescence decay time studies *Application Note* http://www.canberra.com/literature/1012.asp

[6] Hamamatsu 2001 Characteristic and use of Si APD (Avalanche Photodiode) *Technical Information* http://sales.hamamatsu.com/assets/applications/SSD/Characteristics_and_use_of_SI_APD.pdf